ISSN 1674-1056
http://cpb.iphy.ac.cn
http://iopscience.iop.org/cpb
中国物理 B
Chinese Physics
中国物理
Chinese Physics B

Ultra-high-density local structure in liquid water

Cheng Yang(杨成), Chuanbiao Zhang(张传彪), Fangfu Ye(叶方富), Xin Zhou(周昕)
Citation: Chin. Phys. B . 2019, 28(11): 116104 . **doi:** 10.1088/1674-1056/ab4710
Journal homepage: http://cpb.iphy.ac.cn; http://iopscience.iop.org/cpb

What follows is a list of articles you may be interested in

A revised jump-diffusion and rotation-diffusion model

Hua Li(李华), Yu-Hang Chen(陈昱沆), Bin-Ze Tang(唐宾泽)
Chin. Phys. B . 2019, 28(5): 056105 . **doi:** 10.1088/1674-1056/28/5/056105

Fractional Stokes-Einstein relation in TIP5P water at high temperatures

Gan Ren(任淦), Ge Sang(桑革)
Chin. Phys. B . 2018, 27(6): 066101 . **doi:** 10.1088/1674-1056/27/6/066101

Atomic pair distribution function method development at the Shanghai Synchrotron Radiation Facility

Xiao-Juan Zhou(周晓娟), Ju-Zhou Tao(陶举洲), Han Guo(郭瀚), He Lin(林鹤)
Chin. Phys. B . 2017, 26(7): 076101 . **doi:** 10.1088/1674-1056/26/7/076101

Local microstructural analysis for $Y_2O_3/Eu^{3+}/Mg^{2+}$ nanorods by Raman and photoluminescence spectra under high pressure

Jin-Hua Wang(王金华), Ze-Peng Li(李泽朋), Bo Liu(刘波), Bing-Bing Liu(刘冰冰)
Chin. Phys. B . 2017, 26(2): 026101 . **doi:** 10.1088/1674-1056/26/2/026101

Using a water-confined carbon nanotube to probe electricity of sequential charged segments of macromolecules

Wang Yu, Zhao Yan-Jiao, Huang Ji-Ping
Chin. Phys. B . 2012, 21(7): 076102 . **doi:** 10.1088/1674-1056/21/7/076102

Ultra-high-density local structure in liquid water*

Cheng Yang(杨成)[1,2,3], Chuanbiao Zhang(张传彪)[4], Fangfu Ye(叶方富)[1,2,5,†], and Xin Zhou(周昕)[2,‡]

[1] *Beijing National Laboratory for Condensed Matter Physics and CAS Key Laboratory of Soft Matter Physics, Institute of Physics, Chinese Academy of Sciences, Beijing* 100190, *China*
[2] *School of Physical Sciences, University of Chinese Academy of Sciences, Beijing* 100049, *China*
[3] *School of Mechanical and Electrical Engineering, Mianyang Normal University, Mianyang* 621000, *China*
[4] *Department of Physics and Electronic Engineering, Heze University, Heze* 274015, *China*
[5] *Songshan Lake Materials Laboratory, Dongguan* 523808, *China*

(Received 10 August 2019; revised manuscript received 18 September 2019; published online 18 October 2019)

We employ multiple order parameters to analyze the local structure of liquid water obtained from all-atom simulations, and accordingly identify three types of molecules in water. In addition to the well-known low-density-liquid and high-density-liquid molecules, the newly identified third type possesses an ultra-high density and over-coordinated H-bonds. The existence of this third type decreases the probability of transition of high-density-liquid molecules to low-density-liquid molecules and increases the probability of the reverse one.

Keywords: water, local structure, inherent structure

PACS: 61.20.Ja, 64.70.Ja **DOI:** 10.1088/1674-1056/ab4710

1. Introduction

Water plays a very important role in daily life and many physical, chemical, and biological processes.[1,2] Although being one of the most common substances on earth, liquid water has many unusual thermodynamic properties. For example, at low temperatures, its isothermal compressibility and isobaric heat capacity increase (rather than decrease) upon cooling.[1] Clarification of the local structure of liquid water is the key of understanding the origin of these anomalies.[3,4] Furthermore, water molecules interact with each other and form a hydrogen-bond (H-bond) network. Any changes of the position or orientation of individual water molecules influence their neighbors strongly, yielding a collective motion in the H-bond network. The dynamic inhomogeneity of this network is also directly related to the local structures of liquid water.[5,6]

It has been proposed that liquid water contain two types of local structures, and accordingly molecules in liquid water can be divided into two types: the high-density-liquid (HDL) and low-density-liquid (LDL), as revealed from the equilibrium distribution of some specific order parameters.[7–9] The HDL's local structure is disorder. There are four neighbors in its first shell and its fifth neighbor inserts into the gap between the first shell and the second shell. However, the local structure of LDL is ice-like with the fifth neighbor in the second shell. The presence of such two types can explain well the aforementioned unusual thermodynamic properties of water, and is thus widely accepted.[1,3] Here we perform all-atom simulations and identify a third type of water molecules, which is characterized by a new type of (real and/or inherent) local structure and, in particular, by an over-coordinated H-bond structure.

2. Methods

The three water models we used are TIP4P/2005,[10] SPC/E,[11] and TIP4P-Ew.[12] All the simulations were performed in isothermal-isobaric (NPT) ensembles, with those of TIP4P/2005 and SPC/E models performed by using the molecular dynamics package LAMMPS[13] and those of TIP4P-Ew by GROMACS.[14] Long-range solvers were used to compute the long-range Coulombic interactions.[15,16] The simulation conformation is called "real structure". To reduce the influence of thermal fluctuations on the local structures in liquid water,[17] we used the conjugate gradient algorithm to minimize the potential energy of the whole system. The molecules conformation obtained in such a way is called "inherent structure".[18] In recent studies, such minimization method has been successfully employed to identify two different local structures of HDL and LDL.[7–9]

The main analyses presented in this article are based on the TIP4P/2005 model. The simulation of this model includes two cases, containing 216 and 4000 molecules, respectively. The temperature of the 216-molecule simulations ranges from 200 K to 300 K. The simulation time is 200 ns at low temperatures. We repeated the simulation seven times at 200 K and 210 K. The shortest run is 100 ns at 300 K. The 4000-molecule simulations were performed at 300 K for 10 ns. The

*Project supported by the Key Research Program of Frontier Sciences of the Chinese Academy of Sciences (Grant No. QYZDB-SSW-SYS003) and the National Natural Science Foundation of China (Grant Nos. 11574310 and 11774394).

†Corresponding author. E-mail: fye@iphy.ac.cn
‡Corresponding author. E-mail: xzhou@ucas.ac.cn

© 2019 Chinese Physical Society and IOP Publishing Ltd

simulations for the TIP4P-Ew and SPC/E models contain 1000 molecules and were performed at 300 K for 20 ns.

In the simulation, the hydrogen bond is defined based on the distance R_{OO} between the two oxygens in different molecules ($R_{OO} < 0.35$ nm) and the angle θ_{HOO} between the covalent OH and OO bonds ($\theta_{HOO} < 30°$).[19]

The local structure index (LSI) of molecule i, $I(i)$, is defined as follows.[7] Assume the distances (r_j's) between molecule i and its neighbours j's can be sorted as $r_1 < r_2 < r_3 \cdots < r_{n(i)} < 0.37\ \text{nm} < r_{n(i)+1}$, where 0.37 nm sets the starting distance of the second shell; we then have

$$I(i) = \frac{1}{n(i)} \sum_{j=1}^{n(i)} [\Delta(j,i) - \overline{\Delta(i)}]^2, \tag{1}$$

with $\Delta(j,i) = r_{j+1} - r_j$ and $\overline{\Delta(i)}$ denoting the average of $\Delta(j,i)$ over all molecules whose distances to molecule i are less than 0.37 nm. When the local structure is disorder, the value of LSI is close to zero. However, when the local structure is symmetrical, the value of LSI will be much bigger. The LSI has been used successfully in discriminating between HDL and LDL.[7–9]

Let $\boldsymbol{P}(t)$ denote the vector of probabilities of all the states at time t. According to the Chapman–Kolmogorov equation, we can obtain equation $\boldsymbol{P}(t) = \boldsymbol{T}(t)\boldsymbol{P}(0)$, where the matrix $\boldsymbol{T}(t)$ is the transition probability matrix. The transition probability matrix element $T_{ij}(t)$ represents the probability of molecules jumping from state i to state j in time duration t. Assume there are N_1 molecules on state i at time t_0, and N_2 molecules among them jumped to state j at time $t_0 + t$. The ratio between N_2 and N_1 then gives the value of $T_{ij}(t)$. Also, the time evolution of $\boldsymbol{P}(t)$ is governed by equation $\dot{\boldsymbol{P}}(t) = \boldsymbol{K}\boldsymbol{P}(t)$, where $\boldsymbol{K}$ is the transition rate matrix. The solution of this equation is $\boldsymbol{P}(t) = \mathrm{e}^{\boldsymbol{K}t}\boldsymbol{P}(0)$. Comparing this solution and the Chapman–Kolmogorov equation, we find that the transition probability matrix $\boldsymbol{T}$ and transition rate matrix $\boldsymbol{K}$ at time t are related by $\boldsymbol{T} = \exp(t\boldsymbol{K})$.[20] The diagonalizable $\boldsymbol{T}$ can be factorized as $\boldsymbol{T} = \boldsymbol{Q}\boldsymbol{\Lambda}\boldsymbol{Q}^{-1}$. Each column of $\boldsymbol{Q}$ is the eigenvector of $\boldsymbol{T}$ and $\boldsymbol{Q}^{-1}$ is the inverse of $\boldsymbol{Q}$. $\boldsymbol{\Lambda}$ is a diagonal matrix containing all the eigenvalues of $\boldsymbol{T}$. The logarithm of $\boldsymbol{T}$, $\log(\boldsymbol{T})$, is equal to $\boldsymbol{Q}\log(\boldsymbol{\Lambda})\boldsymbol{Q}^{-1}$. Then we can obtain the transition rate matrix $\boldsymbol{K} = \boldsymbol{Q}\frac{\log(\boldsymbol{\Lambda})}{t}\boldsymbol{Q}^{-1}$.

3. Results

We perform all-atom molecular dynamics simulations for the three microscopic water models at temperatures ranging from supercooled to ambient. By employing multiple order parameters to characterize the (real and/or inherent) local structure of water, we identify the presence of three types of molecules in liquid water: in addition to the well-known HDL and LDL,[21–41] there exists a third type, characterized by an ultra-high density and over-coordinated H-bonds. When the temperature rises, the fraction of this third type increases, from a very small value ($< 1\%$) in the deep supercooled region (200 K) to about 7% at the room temperature (300 K). The ultra-high-density-liquid (UHDL) molecules are surrounded by HDL molecules and distribute discretely in space. They decrease the probability of transition of the HDL molecules to LDL molecules and increase the probability of the reverse one, thus leading to the enhancement of the stability of the HDL molecules.

3.1. A new local structure

We start with observing the distributions of r_5 in the inherent structure for different temperatures (Fig. 1(a)), different pressures (Fig. 1(b)), and different water models (Fig. 1(c)). All the distributions have two peaks. The position of the left peak is smaller than $r_5 = 0.3$ nm, and that of the right peak varies slowly with the temperature or pressure. It is worth noting that the distributions obtained from different water models are almost the same, which proves that our results are independent of models. As shown in Appendix A, the bimodal characteristic of the distribution of r_5 can also be observed in the real structure.

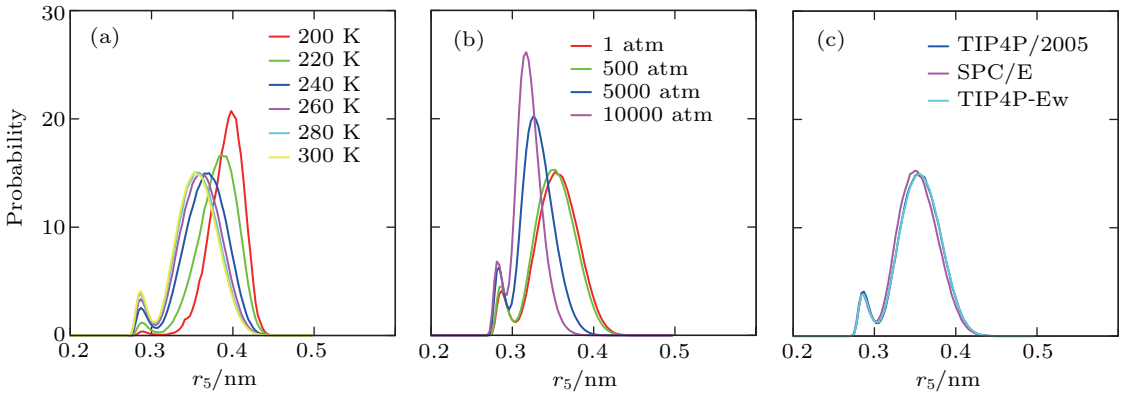


Fig. 1. Distributions of r_5 in the inherent structure for different temperatures, different pressures, and different water models: (a) distributions of r_5 in the inherent structure at different temperatures, calculated from the 216-molecule simulations at 1 atm; (b) distributions of r_5 at different pressures, obtained by the 4000-molecule simulations at 300 K; (c) distributions of r_5 for different models, given by the 1000-molecule simulations at 300 K and 1 atm.

To characterize the local structures in liquid water clearly, we calculate the joint distribution of r_5 and LSI in the inherent structure. As shown in Fig. 2(a), for water at 1 atm and 300 K, there exist three peaks, indicating the presence of three types of local structures of liquid water. The upper right peak, with large LSI and large r_5, corresponds to the LDL structure.[7] Among the two peaks with small LSI, the upper left one, with larger r_5 and much larger height, consists the main part of the low-LSI component,[7] and should thus correspond to the HDL structure; the lower left peak, with the smallest height, has the smallest r_5, representing a local structure with density even higher than that of HDL, i.e., the ultra-high-density liquid (UHDL). Note that the bimodal characteristic of the UHDL peak is caused by the fluctuation of the sixth neighbor around the cutoff at 0.37 nm. The projection of the joint distribution on the vertical axis goes back to the result in Fig. 1.

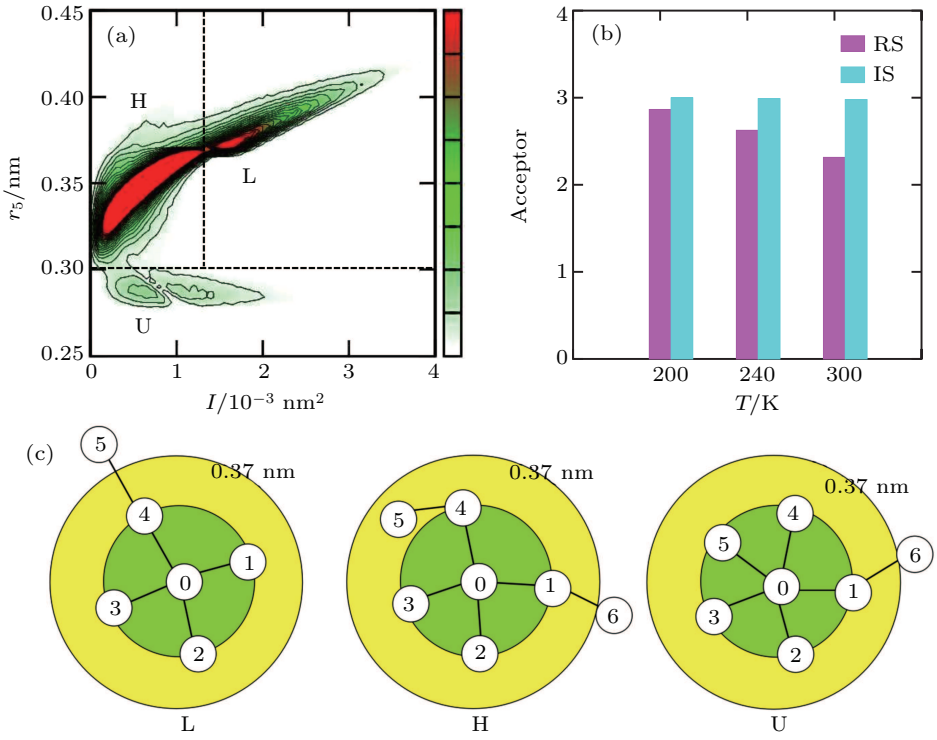


Fig. 2. Identification and characteristics of the third type water molecules. (a) Joint I–r_5 distribution at 1 atm and 300 K in the inherent structure, where the values of the probability density are given by the color bar on the right. The three peaks corresponding to LDL, HDL, and UHDL have been labeled with L, H, and U, respectively. The boundary between the UHDL and HDL is $r_5 = 0.305$ nm and the boundary between the HDL and LDL is $I = 1.35 \times 10^{-3}$ nm^2. (b) Average number of acceptor bonds of UHDL at various temperatures. In the inherent structure, the acceptor bond number is always close to three at all temperatures; in the real structure, due to thermal fluctuation, the acceptor bond number decreases when the temperature increases, but still remains bigger than two even at 300 K. (c) Schematic illustration of three species in the inherent structure, where the fifth neighbor of the LDL molecule locates beyond the 0.37 nm circle and that of the HDL molecule is in the gap between the first and second shells, while the UHDL molecule has five neighbors in the first shell.

We proceed to investigate the H-bond structure of UHDL molecules. Figure 2(b) shows the average number of the acceptor bonds of UHDL at different temperatures: in the inherent structure, the average acceptor bond number is always 3 at all temperatures; while in the real structure, due to the thermal fluctuation, the average acceptor bond number of the corresponding UHDL molecules decreases gradually, but remains much bigger than two even at 300 K. Normally, water molecules have only two acceptors, but UHDL molecules have more than two. That is why we say the UHDL molecules are over-coordinated.

A schematic illustration showing the differences between the LDL, HDL, and UHDL is given in Fig. 2(c) (i) LDL is ice-like, with the fifth neighbor locating beyond the 0.37 nm cutoff circle; (ii) HDL has four neighbors in the first shell, and the fifth neighbor is in the gap between the first and second shells; (iii) UHDL, however, has five neighbors in the first shell, with no molecule in the gap. The LDL and HDL structures are consistent with the descriptions in Ref. [1]. Note that UHDL is different from the very-high-density amorphous ice (VHDA), which has four neighbors in the first shell and two interstitial molecules.[42]

3.2. Roles of UHDL molecules

We label each molecule in the simulations according to its inherent structure. We next discuss the roles of the UHDL molecules. To this end, we first analyze the spatial correlations between the LDL, HDL, and UHDL molecules. Figure 3(a) gives a snapshot of liquid water at 300 K and 1 atm, where the green, white, and red spheres represent the oxygen atoms of LDL, HDL, and UHDL molecules, respectively. As shown in Fig. 3(a), the LDL and HDL molecules prefer to cluster

with the same species, but the UHDL molecules are dispersed among the HDL. In order to confirm this observation, we calculate the percentage of species β in the first-shell neighbors of specie-α molecules, $C_{\alpha\beta}$, where α and β represent LDL, HDL, or UHDL (abbreviated as L, H, and U, respectively), and the concentration of species α in the whole system, C_α. By definition, we have $\sum_\alpha C_\alpha = 1$ and $\sum_\beta C_{\alpha\beta} = 1$. If $C_{\alpha\beta}$ is larger than C_β, species α and β attract each other; otherwise,α and β repel each other. Figures 3(b) and 3(c) give, respectively, the values of the three C_α and the three $C_{\alpha\mathrm{U}}$ at 1 atm and various temperatures between 200 K and 300 K, from which we can clearly see that HDL molecules attract UHDL molecules while the LDL molecules repel UHDL (because $C_{\mathrm{HU}} > C_{\mathrm{U}} > C_{\mathrm{LU}}$). The C_{UU} is smaller than C_{U}, indicating that the UHDL molecules do not tend to form clusters. These two results together suggest that UHDL molecules probably serve as the clustering nuclei of HDL molecules.

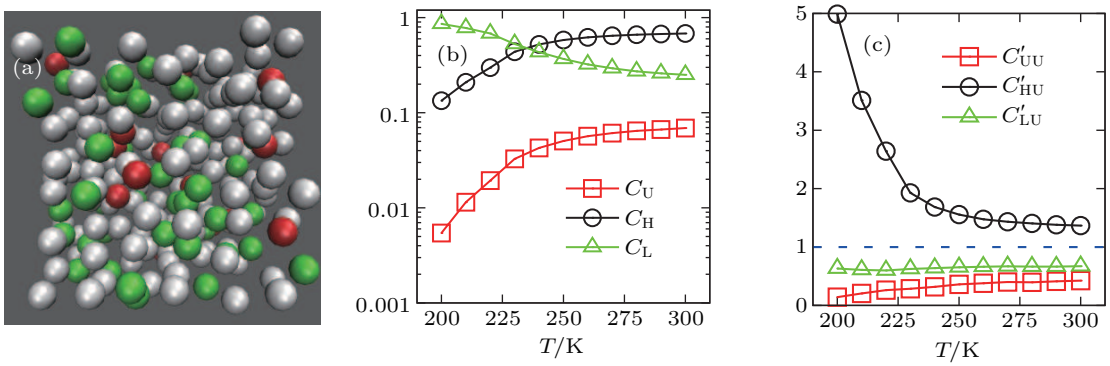


Fig. 3. Concentrations (C_α) of and correlations ($C_{\alpha\beta}$) between different molecule types. (a) Simulation snapshot of 216 liquid-water molecules at 1 atm and 300 K, where the green, white, and red spheres represent the LDL, HDL, and UHDL molecules, respectively. These molecules are labeled according to their inherent local structures. Panels (b) and (c) show, respectively, the temperature dependence of C_α and $C'_{\alpha\mathrm{U}} = C_{\alpha\mathrm{U}}/C_{\mathrm{U}}$ at 1 atm, as given by the 216-molecule simulations.

The existence of UHDL also influences the transitions between the HDL and LDL molecules. To quantify such influences, we compare the transition matrix elements, T_{HL} (representing the probability of transition from the HDL to LDL) and T_{LH} (from LDL to HDL), of the molecules that are in the first shell of UHDL with those of the molecules that are not. As shown in Figs. 4(a) and 4(b), the HDL molecules in the first shell of the UHDL have a lower probability of jumping to LDL, and the first-shell LDL molecules have a higher probability of jumping to HDL, than their non-first-shell counterparts. In another word, the existence of UHDL makes its surrounding HDL more stable and LDL less stable.

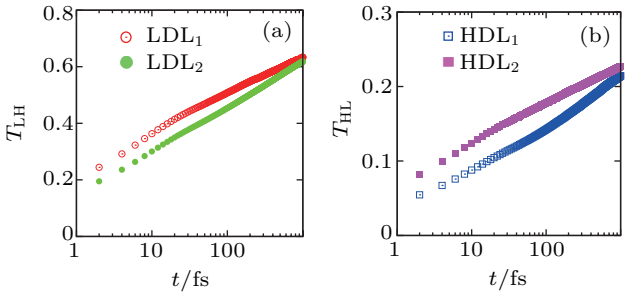


Fig. 4. Transition matrix elements. Panels (a) and (b) show, respectively, the T_{LH} (the transition probability from L to H) and T_{HL} (the transition probability from H to L) at 1 atm and 300 K, given by the 4000-molecule simulations, where the open squares (circles) represent the HDL (LDL) molecules in the first shell of UHDL (HDL_1 and LDL_1) and the solid squares (circles) represent the non-first-shell HDL (LDL) molecules (HDL_2 and LDL_2).

All the transition probabilities and the corresponding transition rates between the different local structures are given in Fig. 5. The transition rate represents how fast one water molecule jumps from one state to another state. If the transition rate from a state to another is much faster than that between other states (orders of magnitude), then the stability of this metastable state is worse than that of the other states, so this metastable state is generally not treated the same as other states. As shown in Fig. 5(b), the transition rate from UHDL to HDL is of the same order as that from LDL to HDL, indicating that UHDL is a stable local structure.

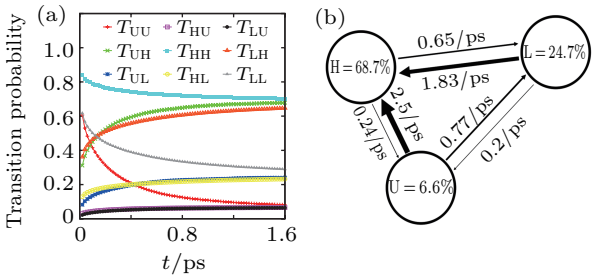


Fig. 5. (a) Transition probabilities (obtained by the 4000-molecule simulations at 300 K and 1 atm) and (b) transition rates between the different local structures, where the numbers in the circles in (b) represent the concentrations of the corresponding species. The convergent transition rates are obtained from the transition probability matrix at $t = 0.8$ ps.

4. Conclusion

We predicted the existence of a third type of molecules (UHDL) in liquid water by investigating its inherent structures, and its main characteristic remains in the real structure. One distinctive feature of such molecules is their over-

coordinated H-bond structure, i.e., the existence of three acceptor bonds. The UHDL molecules disperse in space and are usually surrounded by HDL molecules. The existence of UHDL makes the HDL in contact more stable and LDL in contact less stable. The heterogeneity of liquid water is therefore greatly enhanced. Moreover, although the fraction of the UHDL molecules itself may be small, the fraction of their HDL/LDL neighbors can reach $\sim 35\%$ (the proportion of UHDL molecules is $\sim 7\%$ and each UHDL molecule has five neighbors, so the proportion of the neighbors of UHDL is $\sim 7\% \times 5$) under ambient conditions. In this sense, the presence of UHDL has bigger influence than what its small fraction seemingly means. Its potential influence on the macroscopic properties of water will be explored in near future.

Appendix A: Real structure

The UHDL can be observed in the real structure at low temperatures. To this end, we trace each water molecule to obtain the single-molecule trajectories, and then calculate the probability distribution of r_5 of the single-molecule trajectories. The corresponding results are presented in Fig. A1(a), in which the black thick line is the distribution obtained by averaging all the single-molecule distributions. Although the averaged distribution is unimodal, a small percentage of the single-molecule distributions have bimodal-peaks, as shown in Fig. A1(b). The positions of the left peak in these distributions clearly show the presence of UHDL.

We also compare the single-molecule trajectories of r_5 and I in the real structure with the counterparts in the inherent structure. As shown in Fig. A2, the energy minimization does not change the trend of the trajectory's variation. At 200 K, the segments of the trajectory around $r_5 = 0.3$ nm can be clearly observed in both the real structure and the inherent structure. At 240 K, the segments at $r_5 \sim 0.3$ nm are much shorter, only several picoseconds. In Figs. A2(e) and A2(j), we show the single-molecule transitions between LDL, HDL, and UHDL. Whether a state belongs to LDL, HDL, or UHDL is determined by its position on the map of the joint I–r_5 distribution, where the boundary between the UHDL and HDL is $r_5 = 0.305$ nm and the boundary between the HDL and LDL is $I = 1.35 \times 10^{-3}$ nm^2. Both single-molecule trajectories keep jumping between different states, implying that the simulation time is long enough for the individual molecules to reach local equilibrium and that the UHDL plateaus are real.

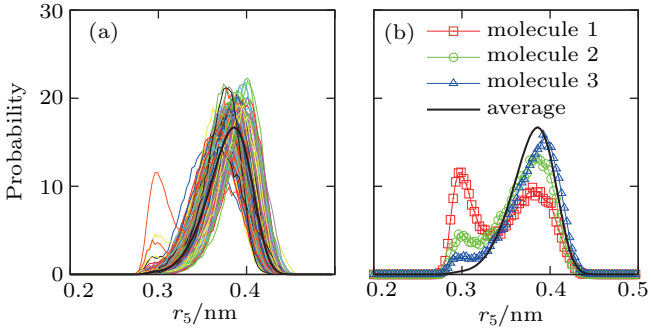


Fig. A1. Distributions of r_5 of single-molecule trajectories in the real structure given by the 216-molecule simulations at 200 K and 1 atm: (a) distributions of all 216 molecules, and (b) distributions of three molecule trajectories showing a bimodal structure, in which the black thick line is the averaged distribution.

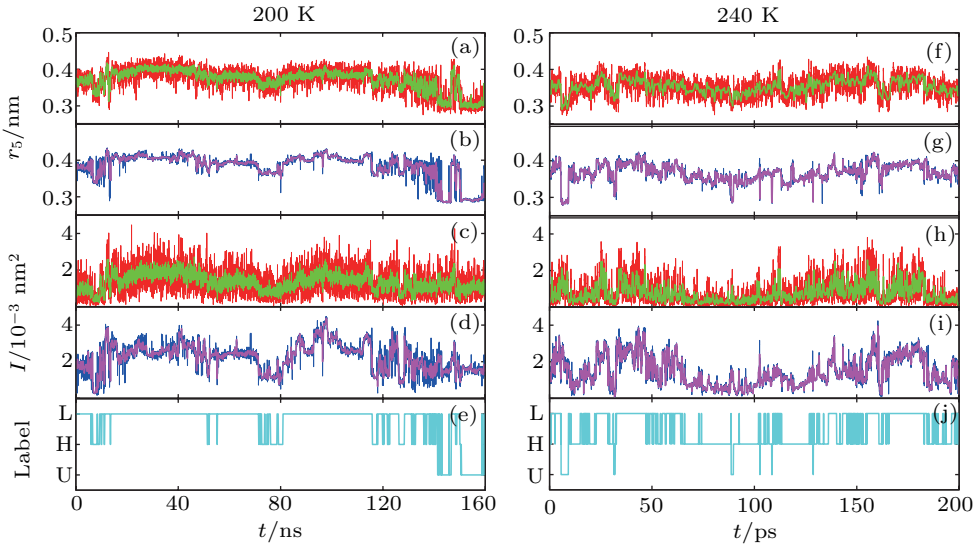


Fig. A2. Single-molecule trajectories in the real and inherent structures: (a) real and (b) inherent r_5 at 200 K, (c) real and (d) inherent I at 200 K, (f) real and (g) inherent r_5 at 240 K, (h) real and (i) inherent I at 240 K, at 1 atm given by the 216-molecule simulations. Panels (e) and (j) show the corresponding transitions of the molecules between the LDL, HDL, and UHDL at 200 K and 240 K, respectively.

We further investigate the influence of the minimization process yielding the inherent structure on the properties of water molecules at low temperatures. We first compute the hydrogen bond numbers and local density (the inverse of the Voronoi polyhedron) of each molecule when they are in the inherent structure, and then compute the corresponding values when they are in the real structure. The comparison of these sets of values are given in Fig. A3, in which the upper row

shows the distributions of LDL, HDL, and UHDL molecules in the inherent structure and the bottom row shows the corresponding distributions in the real structure. The results in the two rows are almost identical, indicating that the minimization process does not obviously change the properties of the water molecules in the super-cooled regime.

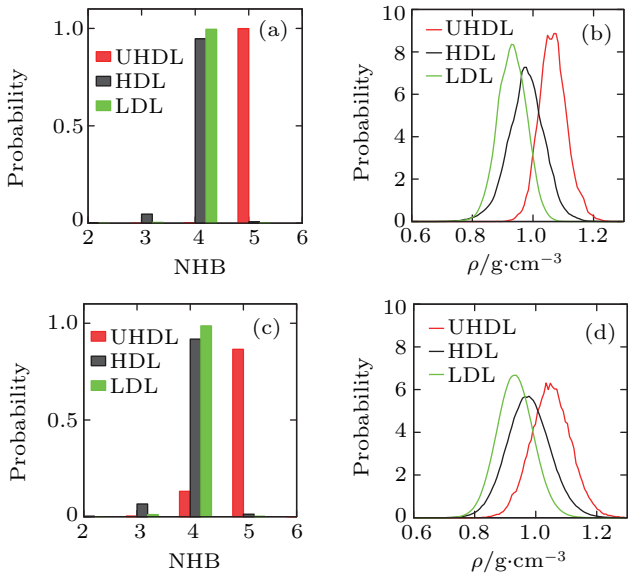


Fig. A3. Distributions of hydrogen-bond numbers (NHB) and local density in the inherent [(a), (b)] and real [(c), (d)] structures, given by the 216-molecule simulations at 200 K and 1 atm.

References

[1] Debenedetti P G 2003 *J. Phys. Condens. Mat.* **15** R1669
[2] Kumar P, Yan Z, Xu L, Mazza M G, Buldyrev S V, Chen S H, Sastry S and Stanley H E 2006 *Phys. Rev. Lett.* **97** 177802
[3] Russo J and Tanaka H 2014 *Nat. Commun.* **5** 3556
[4] Ponyatovsky E G, Sinitsyn V V and Pozdnyakova T A 1998 *J. Chem. Phys.* **109** 2413
[5] Shiratani E and Sasai M 1996 *J. Chem. Phys.* **104** 7671
[6] Matsumoto M, Baba A and Ohmine I 2007 *J. Chem. Phys.* **127** 134504
[7] Wikfeldt K, Nilsson A and Pettersson L G 2011 *Phys. Chem. Chem. Phys.* **13** 19918
[8] Accordino S, Fris J R, Sciortino F and Appignanesi G 2011 *Eur. Phys. J. E* **34** 1
[9] Appignanesi G, Fris J R and Sciortino F 2009 *Eur. Phys. J. E* **29** 305
[10] Abascal J L and Vega C 2005 *J. Chem. Phys.* **123** 234505
[11] Berendsen H, Grigera J and Straatsma T 1987 *J. Phys. Chem.* **91** 6269
[12] Horn H W, Swope W C, Pitera J W, Madura J D, Dick T J, Hura G L and Head-Gordon T 2004 *J. Chem. Phys.* **120** 9665
[13] Plimpton S 1995 *J. Comput. Phys.* **117** 1
[14] Der Spoel D V, Lindahl E, Hess B, Groenhof G, Mark A E and Berendsen H J C 2005 *J. Comput. Chem.* **26** 1701
[15] Pollock E L and Glosli J 1996 *Comp. Phys. Comm.* **95** 93
[16] Essmann U, Perera L, Berkowitz M L, Darden T, Lee H and Pedersen L G 1995 *J. Chem. Phys* **103** 8577
[17] Starr F W, Sastry S, La Nave E, Scala A, Stanley H E and Sciortino F 2001 *Phys. Rev.E* **63** 041201
[18] Debenedetti P G and Stillinger F H 2001 *Nature* **410** 259
[19] Luzar A and Chandler D 1996 *Nature* **379** 55
[20] Noe F and Fischer S 2008 *Curr. Opin. Struc. Biol.* **18** 154
[21] Poole P H, Sciortino F, Essmann U and Stanley H E 1992 *Nature* **360** 324
[22] Wernet P, Nordlund D, Bergmann U, Cavalleri M,Odelius M, Ogasawara H, Näslund L, Hirsch T, Ojamäe L and Glatzel P 2004 *Science* **304** 995
[23] Tokushima T, Harada Y, Takahashi O, Senba Y, Ohashi H, Pettersson L G, Nilsson A and Shin S 2008 *Chem. Phys. Lett.* **460** 387
[24] Huang C, Wikfeldt K T, Tokushima T, Nordlund D, Harada Y,Bergmann U, Niebuhr M, Weiss T, Horikawa Y and Leetmaa M 2009 *Proc. Natl. Acad. Sci. USA* **106** 15214
[25] Paolantoni M, Lago N F, Albertí M and Lagana A 2009 *J. Phys. Chem. A* **113** 15100
[26] Nilsson A and Pettersson L G 2011 *Chem. Phys.* **389** 1
[27] Nilsson A, Huang C and Pettersson L G 2012 *J. Mol. Liq.* **176** 2
[28] Pallares G, Azouzi M E M, González M A, Aragones J L, Abascal J L, Valeriani C and Caupin F 2014 *Proc. Natl. Acad. Sci. USA* **111** 7936
[29] Abascal J L and Vega C 2010 *J. Chem. Phys.* **133** 234502
[30] Kesselring T, Franzese G, Buldyrev S, Herrmann H and Stanley H E 2012 *Sci. Rep.* **2** 474
[31] Liu Y, Palmer J C, Panagiotopoulos A Z and Debenedetti P G 2012 *J. Chem. Phys.* **137** 214505
[32] Li Y, Li J and Wang F 2013 *Proc. Natl. Acad. Sci. USA* **110** 12209
[33] Giovambattista N 2013 *Liquid Polymorphism* **152** 113
[34] Poole P H, Bowles R K, Saika-Voivod I and Sciortino F 2013 *J. Chem. Phys.* **138** 034505
[35] Palmer J C, Martelli F, Liu Y, Car R, Panagiotopoulos A Z and Debenedetti P G 2014 *Nature* **510** 385
[36] Yagasaki T, Matsumoto M and Tanaka H 2014 *Phys. Rev. E* **89** 020301
[37] Liu D, Zhang Y, Chen C C, Mou C Y, Poole P H and Chen S H 2007 *Proc.Natl. Acad. Sci. USA* **104** 9570
[38] Mallamace F, Branca C, Broccio M, Corsaro C, Mou C Y and Chen S H 2007 *Proc. Natl. Acad. Sci. USA* **104** 18387
[39] Sellberg J A, Huang C, McQueen T, Loh N, Laksmono H, Schlesinger D, Sierra R, Nordlund D, Hampton C and Starodub D 2014 *Nature* **510** 381
[40] Kim K H, Späh A, Pathak H, Perakis F, Mariedahl D, Amann-Winkel K, Sellberg J A, Lee J H, Kim S, Park J, Nam K H, Katayama T and Nilsson A 2017 *Science* **358** 1589
[41] Xu L, Kumar P, Buldyrev S V, Chen S H, Poole P H, Sciortino F and Stanley H E 2005 *Proc. Natl. Acad. Sci. USA* **102** 16558
[42] Finney J L, Bowron D T, Soper A K, Loerting T, Mayer E and Hallbrucker A 2002 *Phys. Rev. Lett.* **89** 205503